Coil design for functional magnetic stimulation of the inspiratory muscles

Ian N. Hsiao, Ph.D., member IEEE, Ercheng Zhu, MD, PhD, Vernon Lin, MD, Ph.D.
Department of Physical Medicine and Rehabilitation, University of California, Irvine, CA
Functional Magnetic Stimulation Laboratory, Spinal Cord Injury/Disorder
Health Care Group, VA Long Beach Health Care System, Long Beach, CA

Abstract - **The purpose of this study was to design a new magnetic coil (MC) for effective functional magnetic stimulation (FMS) of inspiratory muscles in human subjects. Part 1 of the study emphasized on the technical procedure of the coil design, and part 2 demonstrated the efficacy of the resulted coil in producing inspiratory functions. Part 2 is reported in another paper titled "Racetrack magnetic coil for functional magnetic stimulation of the inspiratory muscles – toward magnetic assisted ventilation". The primary goal for the new MC was to maximize nerve activation from T_1 to T_6 spinal nerve roots, and minimize activation of other nerves and muscles. Through the process of coil design, a racetrack shaped MC was conceptualized and produced.**

Keywords: **inspiratory muscle, assisted ventilation, magnetic stimulation.**

I. INTRODUCTION

Magnetic stimulation has been used in recent years as a noninvasive method for stimulating the nerves. In recent years, investigators have used magnetic stimulation to evaluate the respiratory system by stimulating the phrenic nerves [1]-[2] and thoracic spinal nerves [3]. In addition, studies have demonstrated significant inspired volume generation by FMS of the inspiratory muscles as well as significant expired pressure production by FMS of the lower thoracic nerves in dogs [4] and significant improvements in expired function in patient with SCI [5]. Furthermore, FMS was applied to restore the impaired expiratory function in SCI patients using a 4-week FMS expiratory muscle training program [6]. After conditioning the expiratory muscles for four weeks, significant improvement in voluntary MEP (16%), FEF (23%) and ERV (73%) was observed.

Conventional round coils in various diameters and winding structures served very well for the stimulation of different muscle groups, for example detrusor muscles [7] and expiratory muscles [5]-[6]. With regard to inspiratory muscle stimulation, these coils were found ineffective in producing meaningful pulmonary function in our preliminary tests in human subjects and, more often than not, the results were inconsistent [3]. The reason may be that the rigorous contraction in shoulder, arm, and back muscles or even expiratory muscles during magnetic stimulation interfered with inspiratory muscle movements during inhalation. The need for designing a MC to selectively stimulate inspiratory muscles while minimizing activation of other muscle groups is apparent.

II. MATERIALS AND METHODS

*A. Experimental **E** Measurements*

The induced **E** in the proximity of the MC was systematically mapped for the new coils. The field probes were a bi-polar probe manufactured in our laboratory and a gaussmeter probe (TBL STE92-0404). The MC was placed below a plastic container with dimensions of 90x60x30 cm. The container was filled with a resistive saline solution approximately equal to that of human tissue, e.g., 500 ohm-cm. The bipolar electric field probe was placed into the saline filled plastic container located directly above the MC. The electrodes of the probe were 0.1cm apart and insulated everywhere except at their tips. The signal generated from this probe was displayed and digitized by an oscilloscope (HP 54602) and synchronized with the reading obtained from the gaussmeter (TBL 9200). The data was then stored in a PC for data analysis. This data included on-screen visualization of the field distribution along a given plane.

The electric field measurements were made when the magnetic stimulation parameters were fixed at 20% of maximal intensity and 20Hz frequency. In order to measure $\partial V_y / \partial y$ with respect to the MC, the two electrodes (1 and 2) of the electric field probe were placed parallel to the y axis. The probe was then moved along the x axis to measure **E**. The voltage sensed at electrode 1, V_1, minus the voltage sensed at electrode 2, V_2, became the voltage difference, ΔV_{12}, between the two electrodes. This was monitored by inserting the two electrodes into channels 1 and 2 of the oscilloscope. If the distance, d, between points 1 and 2 was small, $\partial V_y/\partial y$ at the mid-point between the two electrodes could be approximated as $\Delta V_{12}/d$. Furthermore, changes in $\partial V_y/\partial y$ along the z axis (vertical to the coil plane) were measured at the center of the coil.

B. Computer modeling of magnetic coils

A computer program FlexPDE, developed by PDE Solution, was used to simulate the induced electric field and nerve activation function generated in saline solution. FlexPDE is a general solver for the solutions of systems of partial differential equations such as heat and Maxwell's equations. This solver incorporated a numerical technique based on the finite element method to solve unknowns such as induced electrical fields. To arrive at solutions for the electric field component E_y (y is the orientation of nerve) induced by magnetic stimulation, Maxwell's equations (Eq. 1 a-d) were simplified in the following manner:

$$\nabla \times E = -j\omega\mu H \quad (1a)$$

$$\nabla \times H = J + j\omega\varepsilon E \quad (1b)$$

Report Documentation Page

Report Date	Report Type	Dates Covered (from... to)
25OCT2001	N/A	-

Title and Subtitle Coil design for functional magnetic stimulation of the inspiratory muscles	**Contract Number**
	Grant Number
	Program Element Number
Author(s)	**Project Number**
	Task Number
	Work Unit Number
Performing Organization Name(s) and Address(es) Department of Physical Medicine and Rehabilitation, University of California, Irvine, CA	**Performing Organization Report Number**
Sponsoring/Monitoring Agency Name(s) and Address(es) US Army Research, Development & Standardization Group (UK) PSC 802 Box 15 FPO AE 09499-1500	**Sponsor/Monitor's Acronym(s)**
	Sponsor/Monitor's Report Number(s)

Distribution/Availability Statement
Approved for public release, distribution unlimited

Supplementary Notes
Papers from the 23rd Annual International Conference of the IEEE Engineering in Medicine and Biology Society, October 25-28, 2001, held in Istanbul, Turkey. See also ADM001351 for entire conference on cd-rom., The original document contains color images.

Abstract

Subject Terms

Report Classification unclassified	**Classification of this page** unclassified
Classification of Abstract unclassified	**Limitation of Abstract** UU

Number of Pages
4

$$\nabla \cdot E = \rho/\varepsilon \quad (1c)$$

$$\nabla \cdot H = 0 \quad (1d)$$

Curling both sides of Eq. 1a and combining with Eq. 1b, if the medium is single and uniform then we have

$$\nabla \times \nabla \times E = \nabla \times (-j\omega\mu H) = -j\omega\mu \nabla \times H = -j\omega\mu(J + j\omega\varepsilon E) \quad (2)$$

$$\nabla(\nabla \cdot E) - \nabla^2 E = -j\omega\mu J + \omega^2 \mu\varepsilon E \quad (3)$$

With ρ = 0, assuming no charge source, Eq. 3 becomes

$$\nabla^2 E - j\omega\mu J + \omega^2 \mu\varepsilon E = 0 \quad (4)$$

Separate the real part and imaginary part of $\boldsymbol{E}$ and $\boldsymbol{J}$ as $\boldsymbol{E} = E_r + jE_i$ and $\boldsymbol{J} = J_r + jJ_i$ or $\sigma E_r + \sigma jE_i$ and bring them into Eq. 4

$$\nabla^2(E_r + jE_i) - j\omega\mu\sigma(E_r + jE_i) + \omega^2\mu\varepsilon(E_r + jE_i) = 0 \quad (5)$$

Equate the real part and imaginary part of Eq. 5 separately to 0

$$\nabla^2 E_r + \omega\mu\sigma E_i + \omega^2 \mu\varepsilon E_r = 0 \quad (6a)$$

$$\nabla^2 E_i - \omega\mu\sigma E_r + \omega^2 \mu\varepsilon E_i = 0 \quad (6b)$$

Equations 6a and 6b can be simplified to a 2-dimensional problem in the case of a round coil. However, if the coil is not round, such as a racetrack coil, the problem is then a 3-dimensional one. Since the primary variables of interest are $E_{i,x}$ and $E_{i,y}$, E_z is neglected and Eq. 6a and 6b are reduced to the following equations,

$$\partial^2(E_{r,x})/\partial x^2 + \partial^2(E_{r,x})/\partial y^2 + \partial^2(E_{r,x})/\partial z^2 + \omega\mu\sigma E_{i,x} + \omega^2\mu\varepsilon E_{r,x} = 0 \quad (7a)$$

$$\partial^2(E_{i,x})/\partial x^2 + \partial^2(E_{i,x})/\partial y^2 + \partial^2(E_{i,x})/\partial z^2 - \omega\mu\sigma E_{r,x} + \omega^2\mu\varepsilon E_{i,x} = 0 \quad (7b)$$

$$\partial^2(E_{r,y})/\partial x^2 + \partial^2(E_{r,y})/\partial y^2 + \partial^2(E_{r,y})/\partial z^2 + \omega\mu\sigma E_{i,y} + \omega^2\mu\varepsilon E_{r,y} = 0 \quad (7c)$$

$$\partial^2(E_{i,y})/\partial x^2 + \partial^2(E_{i,y})/\partial y^2 + \partial^2(E_{i,y})/\partial z^2 - \omega\mu\sigma E_{r,y} + \omega^2\mu\varepsilon E_{i,y} = 0 \quad (7d)$$

For the purpose of computer modeling, the fourth term of Eq. 7b and 7d can be rewritten as $-\omega\mu(\sigma E_{r,x} + J_{r,x})$ and $-\omega\mu(\sigma E_{r,y} + J_{r,y})$, respectively, to account for the operating current in the coils. $J_{r,x}$ and $J_{r,y}$ are the current density in the coil region in the computer model in perspective direction, and they are 0 everywhere else.

Solving a problem with FlexPDE required physical description of the problem. To describe the problem, it was necessary to define the boundaries, place the material properties in appropriate regions, and assign the excitations and operation frequency. The current I in the coils was set randomly at a magnitude of 10000A and frequency of 5000Hz in all the computer modeling. A single uniform medium, saline, was assumed in the modeling. A 3-D model and a 2-D were constructed to model the coils. Two coils as shown in Fig. 1, a round 12.5cm and a racetrack coil (8cmx16cm) were modeled. The current is assumed to be flowing uniformly from the center to the circumference in these coils.

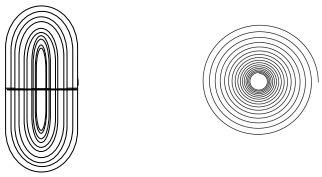

Fig. 1: Geometry of the racetrack coil (left) and round coil (right).

III. RESULTS

A. Electric field measurements

E measurements were plotted for the racetrack 8cmx16cm and round 12.5cm coils. Fig. 2 showed the results of the measured electric field (E_y, parallel to nerve orientation) distribution taken at successive intervals of 0.5cm along the line y = 0.0cm, starting at the center (x = 0.0cm) of the coil to x = 8cm. Both coils had zero field intensity at the center of the coils (x = 0.0cm), and the field intensity increased to a peak of 63.9 and 79.1 V/m at x = 3.0 and 4.0 cm, respectively. The locations of the peaks were inside the spiral coils rather than at the outer edges of the coils. After their peaks, E_y of the two coils behaved very similarly. E_y of both of the coils gradually decreased to zero with increasing x. Induced E_y was measured at the x = 3.0 and 4.0cm of the coil along the z-axis as shown in Fig. 3. These measurements compared the penetration of the two coils. As seen in Fig. 2, the round 12.5cm coil had a higher initial field strength than the smaller coils at z = 1.0 cm, 79.1 V/m, but it gradually declined with respect to z to 13.6 V/m at z = 6.0cm distance. In contrast, the racetrack 8cmx16cm coil had an initial E_y of 63.9 V/m, which decreased to 14.1 V/m at z = 6.0cm.

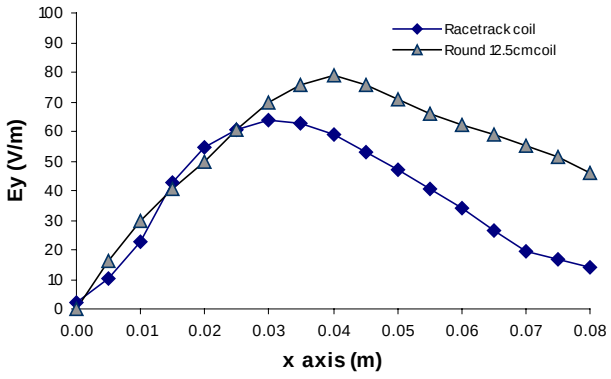

Fig. 2: Electric field strength distribution of the round 12.5cm and the racetrack8cmx16cm coils.

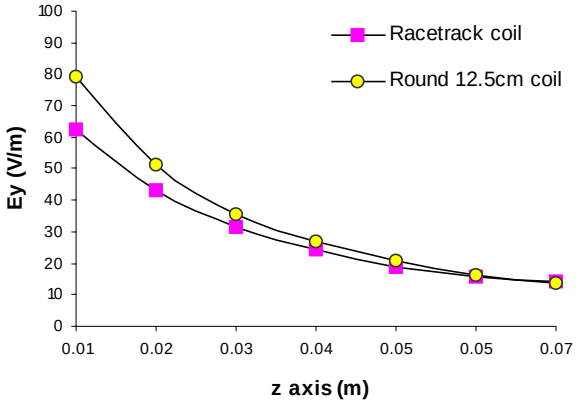

Fig. 3: Penetration of the round 12.5cm and the racetrack 8cmx16cm coils.

B. Computer modeling of magnetic coils

Two coils, the racetrack 8cmx16cm and the round 12.5cm, described above were simulated using FlexPDE models. The computer simulation results of the distributions of induced electric field strength in the y direction, E_y, along the x axis at z = 1cm for the coils were shown in Fig. 4. The computational results displayed the same pattern as those of the experimental results. The peaks of E_y for the two coils were 33.3 and 35.7 V/m at x = 3.25 and 4.25 cm for the round and racetrack coils respectively. Similarly, E_y was computed at the x = 3.25 and 4.25cm of the two coils respectively along the z-axis. The round 12.5cm coil had a slightly lower initial field strength than the racetrack coil at z = 1.0 cm, 33.3 V/m, but it gradually declined with respect to z to 10.5 V/m at z = 7.0cm distance. In contrast, the racetrack 8cmx16cm coil had an initial E_y of 35.7 V/m, which decreased to 12.3 V/m at z = 7.0cm. Furthermore, the computational results of the distribution of $-\partial E_y/\partial y$ along a 45^o line of x axis at z = 1cm for the 12.5cm round coil are shown in Fig. 5. The $-\partial E_y/\partial y$ for the coil had a peak of $-955.0 V/m^2$ at a distance of 6.7cm from the center along a 45^o line with respect to the x axis. From the peak, $\partial E_y/\partial y$ contour lines spread out in all directions and leveled off towards both the x and y axis. The results of $-\partial E_y/\partial y$ distribution were calculated from the 2-D model.

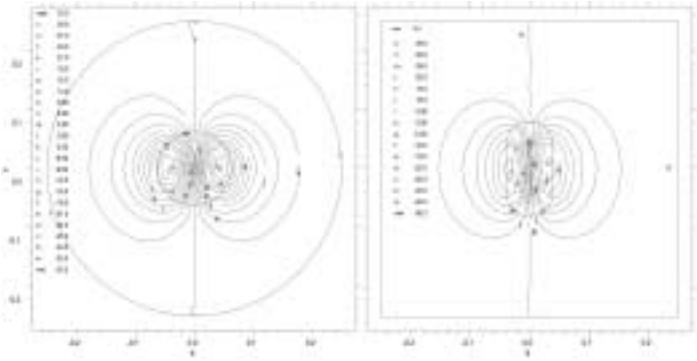

Fig. 4: Contour plots of induced electric field strength vs. coil position: comparison of the round 12.5cm and the racetrack 8cmx16cm coils.

IV. DISCUSSION

The contour lines of the E_y and $-\partial E_y/\partial y$ (nerve activation function [8]-[9]) distributions obtained from computer modeling delineate the possibilities of nerve depolarization in the aperture of the magnetic coils, the spot where the peak of $-\partial E_y/\partial y$ is located being the most probable place of stimulation. The distributions offer a good illustration of a coil's performance in an infinite homogeneous volume conductor where the theory is established, and lend an approximate idea of the distributions in a very complex environment such as the human body. The 12.5cm round coil mapped out a single phase and smooth $-\partial E_y/\partial y$ distribution within and without the perimeter of the coils. The peak of $-\partial E_y/\partial y$ is located at a distance of the coil's radius along the $x\angle 45^o$ line, and $-\partial E_y/\partial y$ decreases gradually from its maximum to 0, toward the x and y axes. The $-\partial E_y/\partial y$ distribution profile points out that the round coil can potentially activate a few groups of muscles besides the upper intercostals muscles, e.g. when placed at T_3. In fact, expiration was actually produced in human subjects [3] using the same stimulator and coil when the coil was placed at $T_1 - T_6$ (coil placement based on the location of center of coil). The reported expiratory pressure ranged from 23 (placed at T_1) to 31 (T_6) cmH_2O, and expiratory volumes from 0.4 (T_1) to 0.7 (T_6) L. This probably was caused by the excessive expiratory functions produced by the round 12.5cm coils, even though inspiratory functions were also produced at the same time. It is clear that an appropriate coil needs to be designed for the successful generation of inspiratory function by FMS.

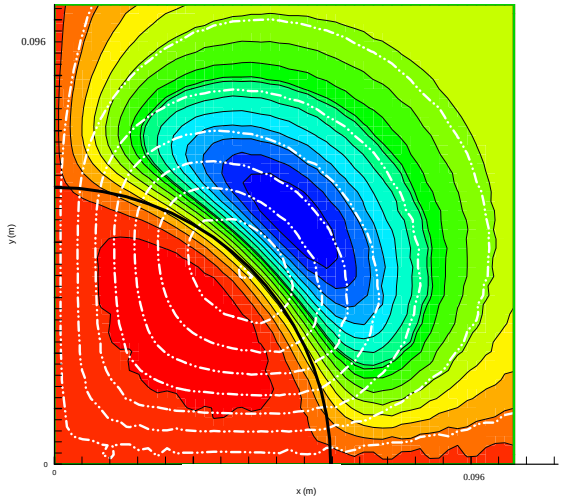

Fig. 5: Contour plots of nerve activation function strength: comparison of the round 12.5cm coil (computational results, gray levels refer to the round coils, gray levels black represents extreme values and that white corresponds to 0; white lines to the round coil).

The goal of the design is to simultaneously stimulate T_1 to T_6 spinal nerves that innervate the inspiratory muscles, and minimally activate other nerves and muscles. Since the round coil stimulates unwanted nerves besides the targeted nerves, logically the coil shape of choice would be a racetrack shape with a longitudinal span covering T_1 to T_6. Checking with the $-E_y$ distribution in the racetrack shaped coil from the computer model, activation becomes weak outside of the coil periphery. Therefore, the length of the racetrack coil can be set at 16cm, which is about the average length from T_1 to T_6 of the subjects in this study. Ideally, limiting the width of the coil to the vicinity of neuroforamina (2 ~ 3cm from the middle line of the spine) is a good choice to avoid superfluous nerve activation and to make sure that T_1 to T_6 spinal nerves are covered. However, the size of the coil is restricted by the fact that smaller MCs produce lower stimulation strengths [10]. To compromise, a midpoint width of 8cm is adopted. The measured E_y of the racetrack coil is indeed weaker than that of the 12.5cm round coil, as shown in Fig. 2. Fig. 2 also shows that the peak of E_y is at x = 3.0cm for the racetrack coil rather than at x = 4.0cm as it is for the round coil. Therefore, the racetrack coil is expected to limit stimulation to a narrower area than the round coil. The computer modeling results of E_y and $-\partial E_y/\partial y$ distributions in Fig. 2 through 5 demonstrate the same point.

V. CONCLUSION

FMS has gradually gained popularity in the areas of neuromuscular diagnostics and rehabilitation in recent years. Magnetic coil design is one of the most important aspects of the FMS technique for its application in clinical settings. This is because different clinical applications often times require different stimulation patterns. One well-known example was to design coils for focal stimulation. The present study is intended to address the incapability of the round coils in producing inspiratory functions. The outcome of the study, a racetrack shaped coil, may provide a solution to the challenge. This coil will be tested in human in the next part of the study.

ACKNOWLEDGMENTS

The authors thank Jane Babbitt, MS, Kathie Kim, MPH, and David Liu, BS for their support and assistance at various stages of this project. This project was supported in part by grants from National Institute of Child Health and Human Development (Grant # HD36917) and VA Rehabilitation Research and Development Service.

REFERENCES

[1] GH Mills, D. Kyroussis, CH. Hamnegard, S. Wragg, J. Moxham, M Green. Unilateral magnetic stimulation of the phrenic nerve. Thorax. 50(11):1162-72, 1995.

[2] GH Mills, D. Kyroussis, CH. Hamnegard, S. Wragg, MI. Polkey, J. Moxham, M. Green. Cervical magnetic stimulation of the phrenic nerves in bilateral diaphragm paralysis. Am. J. Respir. Crit. Care. Med. 155(5):1565-9, 1997.

[3] H Singh, M Magruder, T Bushnik, V Lin. Expiratory muscle activation by functional magnetic stimulation of thoracic and lumbar spinal nerves. Crit. Care Med. 27(10):2201-5, 1999.

[4] VWH Lin, JR Romaniuk, AF. DiMarco. Functional magnetic stimulation of the respiratory muscles in dogs. Muscle & Nerve. 21(8):1048-57, 1998.

[5] VWH Lin, H. Singh, RK. Chitkara, I. Perkash. Functional magnetic stimulation for restoring cough in patients with tetraplegia. Arch. Physic. Med. & Rehabil. 79(5):517-22, 1998.

[6] VWH Lin, IN Hsiao, E. Zhu, I. Perkash. Functional magnetic stimulation for conditioning of expiratory muscles in patients with spinal cord injury. Arch. Physic. Med. & Rehabil. 82(2):162-166, 2001.

[7] VWH Lin, V Wolfe, I Perkash. Micturition by functional magnetic stimulation. J Spinal Cord Med 20:218-226, 1997.

[8] B.J. Roth, P.J. Basser. "A model of the stimulation of a nerve fiber by electromagnetic induction", IEEE TBE, vol. 37, pp. 588-597, 1990.

[9] J. Nilsson, M. Panizza, B.J. Roth et al. "Determining the site of stimulation during magnetic stimulation of the peripheral nerve", Electroencephalographs and clinical neurophysiology. vol 85, pp. 253-264, 1992.

[10] VWH Lin, IN Hsiao, V Dhaka. Magnetic coil design considerations for functional magnetic stimulation. IEEE Transactions on Biomedical Engineering. 47(5):600-610, 2000.